01 Nov 2018

Bio-Inspired Polydopamine Surface Modification of Nanodiamonds and its Reduction of Silver Nanoparticles

Yun Zeng

Wenyan Liu
Missouri University of Science and Technology, liuweny@mst.edu

Risheng Wang
Missouri University of Science and Technology, wangri@mst.edu

Recommended Citation

Y. Zeng et al., "Bio-Inspired Polydopamine Surface Modification of Nanodiamonds and its Reduction of Silver Nanoparticles," *Journal of Visualized Experiments*, vol. 2018, no. 141, Journal of Visualized Experiments, Nov 2018.
The definitive version is available at https://doi.org/10.3791/58458

Video Article

Bio-inspired Polydopamine Surface Modification of Nanodiamonds and Its Reduction of Silver Nanoparticles

Yun Zeng[1], Wenyan Liu[2], Risheng Wang[1]

[1]Department of Chemistry, Missouri University of Science and Technology

[2]Center for Research in Energy and Environment, Department of Chemistry, Missouri University of Science and Technology

Correspondence to: Risheng Wang at wangri@mst.edu

URL: https://www.jove.com/video/58458
DOI: doi:10.3791/58458

Keywords: Chemistry, Issue 141, Nanodiamonds, polydopamine, reduction, silver nanoparticles, surface modification, self-polymerization.

Date Published: 11/14/2018

Citation: Zeng, Y., Liu, W., Wang, R. Bio-inspired Polydopamine Surface Modification of Nanodiamonds and Its Reduction of Silver Nanoparticles. *J. Vis. Exp.* (141), e58458, doi:10.3791/58458 (2018).

Abstract

Surface functionalization of nanodiamonds (NDs) is still challenging due to the diversity of functional groups on the ND surfaces. Here, we demonstrate a simple protocol for the multifunctional surface modification of NDs by using mussel-inspired polydopamine (PDA) coating. In addition, the functional layer of PDA on NDs could serve as a reducing agent to synthesize and stabilize metal nanoparticles. Dopamine (DA) can self-polymerize and spontaneously form PDA layers on ND surfaces if the NDs and dopamine are simply mixed together. The thickness of a PDA layer is controlled by varying the concentration of DA. A typical result shows that a thickness of ~5 to ~15 nm of the PDA layer can be reached by adding 50 to 100 µg/mL of DA to 100 nm ND suspensions. Furthermore, the PDA-NDs are used as a substrate to reduce metal ions, such as $Ag[(NH_3)_2]^+$, to silver nanoparticles (AgNPs). The sizes of the AgNPs rely on the initial concentrations of $Ag[(NH_3)_2]^+$. Along with an increase in the concentration of $Ag[(NH_3)_2]^+$, the number of NPs increases, as well as the diameters of the NPs. In summary, this study not only presents a facile method for modifying the surfaces of NDs with PDA, but also demonstrates the enhanced functionality of NDs by anchoring various species of interest (such as AgNPs) for advanced applications.

Video Link

The video component of this article can be found at https://www.jove.com/video/58458/

Introduction

Nanodiamonds (NDs), a novel carbon-based material, have attracted considerable attention in recent years for use in various applications[1,2]. For instance, the high surface areas of NDs provide excellent catalyst support for metal nanoparticles (NPs) because of their super-chemical stability and thermal conductivity[3]. Furthermore, NDs play significant roles in bio-imaging, bio-sensing, and drug delivery due to their outstanding biocompatibility and nontoxicity[4,5].

To efficiently extend their capabilities, it is valuable to conjugate functional species on the surfaces of NDs, such as proteins, nucleic acids, and nanoparticles[6]. Although a variety of functional groups (*e.g.*, hydroxyl, carboxyl, lactone, *etc.*) are created on the surfaces of NDs during their purification, the conjugation yields of the functional groups are still very low because of the low density of each active chemical group[7]. This results in unstable NDs, which tend to aggregate, limiting further application[8].

Currently, the most common methods used to functionalize NDs, are covalent conjugation by using copper-free click chemistry[9], covalent linkage of peptide nucleic acids (PNA)[10], and self-assembled DNA[11]. The non-covalent wrapping of NDs has also been proposed, including carbohydrate-modified BSA[4], and HSA[12]coating. However, because these methods are time consuming and inefficient, it is desirable that a simple and generally applicable method can be developed to modify the surfaces of NDs.

Dopamine (DA)[13], known as a natural neurotransmitter in the brain, was widely used for adhering and functionalizing nanoparticles, such as gold nanoparticles (AuNPs)[14], Fe_2O_3[15], and SiO_2[16]. Self-polymerized PDA layers enrich amino and phenolic groups, which can be further utilized to directly reduce metal nanoparticles or to easily immobilize thiol/amine-containing biomolecules on an aqueous solution. This simple approach was recently applied to functionalize NDs by Qin *et al*. and our laboratory[17,18], although DA derivatives were employed to modify NDs *via* Click Chemistry in earlier studies[19,20].

Here, we describe a simple PDA-based surface modification method that efficiently functionalizes NDs. By varying the concentration of DA, we can control the thickness of a PDA layer from a few nanometers to tens of nanometers. In addition, the metal nanoparticles are directly reduced and stabilized on the PDA surface without the need for additional toxic reduction agents. The sizes of the silver nanoparticles depend on the initial concentrations of $Ag[(NH_3)_2]^+$. This method allows the well-controlled deposition of PDA on the surfaces of NDs and the synthesis of ND conjugated AgNPs**,** which dramatically extends the functionality of NDs as excellent nano-platforms of catalyst supports, bio-imaging, and bio-sensors.

Protocol

1 . Preparation of Reagents

CAUTION: Please read and understand all relevant material safety data sheets (MSDS) before use. Some of the chemicals are toxic and volatile. Please follow special handling procedures and storage requirements. During the experimental procedure, use personal protective equipment, such as gloves, safety glasses, and a lab coat to avoid potential hazards.

1. Preparation of Tris-HCl buffer
    1. Dissolve 30.29 g of Tris powder in 100 mL of deionized H_2O, ensure that the powder dissolves completely, and then transfer the solution to a 250 mL-volumetric flask.
    2. Add deionized H_2O to the scale of 250 mL in the volumetric flask to give 1.0 M of Tris buffer.
    3. Dilute the 1.0 M Tris buffer 100 times to give 0.01 M Tris buffer and adjust the pH to 8.5 by using 1.0 M HCl standard solution.
    4. Use a pH-meter to calibrate the pH value of the 0.01 M Tris-HCl buffer.

2. Preparation of ND suspensions
    1. Dilute 100 nm of monocrystalline ND suspensions (1.0 mg/mL) 50 times with the 0.01 M Tris-HCl buffer to give 0.02 mg/mL of ND suspensions.

3. Preparation of dopamine solution
    1. Dissolve 20 mg of dopamine hydrochloride in 2.0 mL of 0.01 M Tris-HCl buffer to give 10 mg/mL DA solution.
    NOTE: The DA solution must be freshly prepared and used within 15 min.

4. Preparation of $Ag[(NH_3)_2]OH$ solution
    1. Dissolve 100 mg of $AgNO_3$ solid in 10 mL of deionized H_2O to give 10 mg/mL $AgNO_3$ solution.
    2. Add 1.0 M ammonium hydroxide ($NH_3 \cdot H_2O$) dropwise to the $AgNO_3$ solution until yellow precipitate forms, then continue to add the $NH_3 \cdot H_2O$ solution until the precipitation disappears.
    NOTE: Make the minimum volume required; prepare immediately before use and dispose immediately after use.
    CAUTION: Add $NH_3 \cdot H_2O$ in fume hood with face shields, gloves, and goggles.

2 . Synthesis PDA Layer on the Surface of NDs (PDA-NDs)

1. Add the freshly prepared DA solution (10 mg/mL) to the ND suspensions to give varied final concentrations of 50, 75, 100 μg/mL of DA. Adjust the total reaction volume to 1.0 mL, transfer it to a 10 mL-test tube, and vigorously stir at 25 °C, in the dark for 12 h.
2. Centrifuge the PDA-NDs solution for 2 h at 16,000 x g, remove the supernatant and wash three times with deionized water for 1 h at 16, 000 x g each time.
3. Re-disperse the PDA-NDs in 200 μL of deionized water with sonication for 30 s. The PDA- coated NDs will be ready for further use.

3 . Reduction of AgNPs on the Surface of PDA-NDs (AgNPs-PDA-NDs)

1. Dilute 40 μL of the pre-synthesized PDA-NDs in Step 2.3 two times with deionized water. Add $Ag[(NH_3)_2]OH$ solution to give various final concentrations of $Ag[(NH_3)_2]^+$ (0.08, 0.16, 0.24, 0.40, and 0.60 mg/mL).
2. Adjust the final volume to 100 μL in a 1.5 mL-centrifuge tube by adding deionized water, followed by sonication for 10 min.
3. Centrifuge the AgNPs-PDA-NDs for 15 min at 16,000 x *g* to remove the free silver ions, discard the supernatant after centrifugation, add 100 μL of deionized water, and wash three times with deionized water at 16,000 x *g* for 5 min each time.
4. Re-disperse the AgNPs-PDA-NDs in 100 μL of deionizedwater with sonication for 30 s to prepare for further use.

4 . Analysis of PDA-NDs and AgNPs-PDA-NDs Clusters

1. Ultraviolet-visible (UV) spectra
    1. Use the UV spectra to monitor the average size distribution of AgNPs on PDA-ND surfaces. Transfer the AgNPs-PDA-NDs samples prepared in Step 3.4 with varied concentrations of $Ag[(NH_3)_2]OH$ in 1 cm-quartz cuvette and monitor the absorption at a scan wavelength of 250 to 550 nm.

2. Transmission election microscopy (TEM)
    1. Place the carbon coated copper grids on a glass slide wrapped with parafilm to keep the grids in place. Insert the glass slide with attached TEM grids into the plasma cleaner. Turn on the plasma cleaner and the vacuum pump. After 5 min, turn on the plasma and discharge the grids with a medium power level for 3 min.
    2. Deposit 5 μL of the samples on the carbon film coated Cu-grids for 3 min. Use filter paper to wick off the extra sample from the edge of grid. Then, deposit a drop of deionized water on the grid for 15 s to remove salts, then wick off the water with filter paper. Repeat the washing procedure twice and allow the grid to air dry for further use.
    3. Visualize the samples by TEM, typically at 38,000X magnification. Operate at 200 KV.

Representative Results

The formation of PDA layers on ND surfaces were analyzed by TEM (**Figure 1**). Different thicknesses of PDA layers were observed as higher concentrations of DA led to thicker PDA layers. In addition, after an encapsulating reaction, the color of the NDs solution changed from colorless to dark, while the higher the initial concentration of DA was, the darker the solution became.

Figure 2 describes the reduction of $Ag[(NH_3)_2]^+$ to AgNPs on the surface of 100 nm PDA-ND surfaces. The size distribution of AgNPs, calculated by TEM, were used to determine the dependence of the original concentration of $Ag[(NH_3)_2]^+$ on the sizes of the AgNPs.

The flow chart in **Figure 3** presents the two-step procedure for functionalizing the surface of NDs by PDA and for reducing metal ions into NPs on the PDA-ND layers.

The formation of AgNPs on the ND surface was monitored by UV-vis spectra (**Figure 4**). The intensity of the peaks at ~ 400 nm increased, along with an increase in the concentration of silver solution while the peaks showed a red-shift, indicating the formation of AgNPs with increased sizes.

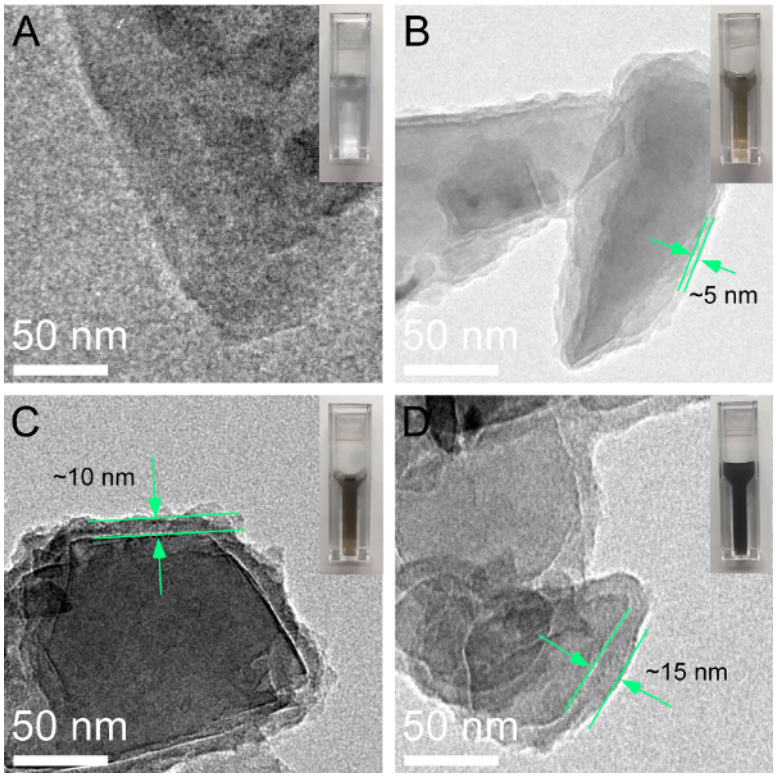

Figure 1. Characterization of the thicknesses of PDA layers on the surfaces of 100 nm NDs with varied concentrations of DA (0, 50, 75, and 100 µg/mL) and their corresponding TEM images. The average thicknesses of each PDA layer are ~5 nm (**B**), ~10 nm (**C**), and ~15 nm (**D**), respectively. The inset photograph shows the colorimetric change in the corresponding samples. Please click here to view a larger version of this figure.

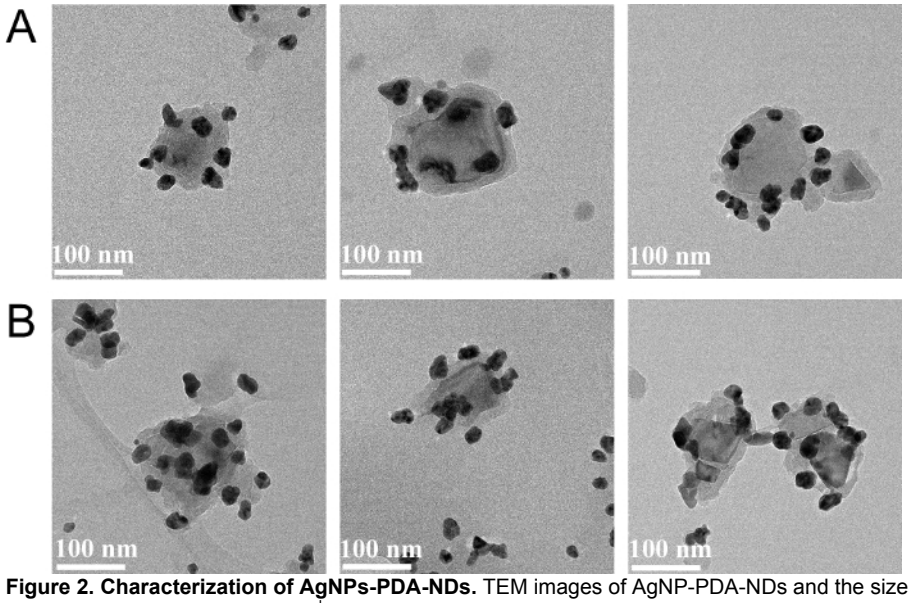

Figure 2. Characterization of AgNPs-PDA-NDs. TEM images of AgNP-PDA-NDs and the size distribution of AgNPs by adding 0.4 mg/mL (**A**), and 0.6 mg/mL (**B**) of $[Ag(NH3)_2]^+$, respectively. Please click here to view a larger version of this figure.

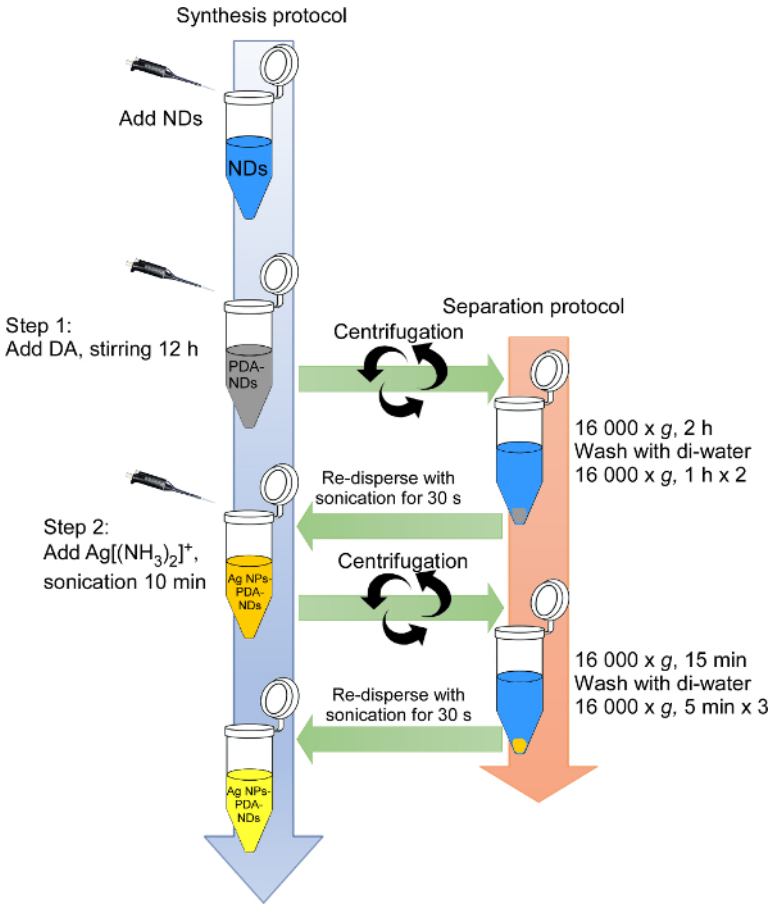

Figure 3. Wall chart diagram of the surface functionalization of NDs. Two-step functionalization of the surface of NDs: (1) the surface coating of NDs with DA polymerization; (2) the reduction of metal ions into NPs on the PDA layer. Please click here to view a larger version of this figure.

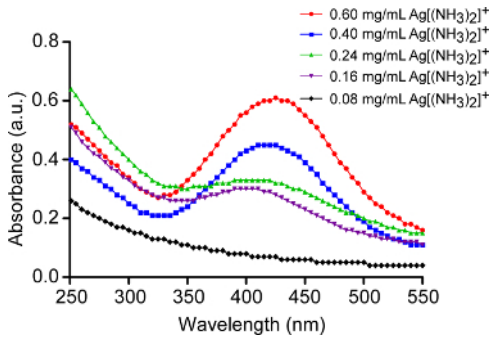

Figure 4. Characterization of reduced AgNPs on the surfaces of NDs, via UV-vis spectroscopy. This figure has been modified and reprinted by permission from Zeng *et al.*[17]. Please click here to view a larger version of this figure.

(1) PDA layer deposition			
Group No.	Initial concentrations of DA (C_1, μg/mL)	Thickness of the PDA layer (d, nm)	Notes:
G_1	50	5	The thickness of PDA layers (d) is directly proportional to the initial concentrations of DA (C_1), and it was discussed in DISCUSSION part.
G_2	75	10	
G_3	100	15	
(2) AgNPs growth synthesis			
Group No.	Initial concentrations of $[Ag(NH_3)_2]^+$ (C_2, mg/mL)	AgNPs average radius (r, nm)	Notes:
G_1	0.4	12	$(Gr_2/Gr_1)^3=(14/12)^3=1.588$ $G_2/G_1=0.6/0.4=1.5$ The ratio of initial concentrations of $[Ag(NH_3)_2]^+$ is consistent with average radius cubed.
G_2	0.6	14	

Table 1. The thickness of PDA layer and the size of reduced AgNPs. The validation of the mathematical models with experimental data. The thickness of PDA layer is determined by the initial concentration of DA, and the ratio of initial concentrations of $[Ag(NH_3)_2]^+$ is consistent with the average radius cubed of AuNPs.

Discussion

This article provides a detailed protocol for the surface functionalization of NDs with self-polymerized DA coating, and the reduction of $Ag[(NH_3)_2]^+$ to AgNPs on PDA layers (**Figure 3**). The strategy is capable of producing various thicknesses of PDA layers by simply changing the concentration of DA. The size of the AgNPs can also be controlled by altering the original concentration of metal ion solution. The TEM image in **Figure 1A** displays the uncoated 100 nm NDs which tended to form microclusters and aggregates. When NDs were encapsulated with PDA, the PDA layers showed as a thin ring round the NDs. The thicknesses of the PDA layers, as measured in TEM images, were around 5 nm, 10 nm, and 15 nm, which corresponded to the final DA concentrations of 50 μg/mL, 75 μg/mL, and 100 μg/mL, respectively. The color of the NDs suspension was observed to change from colorless to dark following PDA coating, indicating the successful wrapping of PDA on ND surfaces and showing that the thickness of PDA was dependent on the concentration of DA. Please note: the critical factor that influences the DA polymerization is the pH condition (the most favorable value is 8.5[23]). The accurate pH value of a solution is beneficial for controlling the thicknesses of PDA layers. In addition, fast agitation during polymerization is necessary for the disaggregation of NDs and the formation of a uniformed PDA layer. Therefore, this method is not effective for any particles that are unstable in alkaline solutions.

To describe the influential factors that contributed to the thickness of the PDA, we introduce **equation (1)** to describe the formation of a PDA layer on ND surfaces. This is based on the kinetic equation of PDA deposition on nanoparticles from previous reports[21,22]. The initial concentrations of DA (C_1, m/v), reaction time (t), and the thickness of the PDA layer (d), are as follows:

$$\frac{4}{3}\pi\rho_1 N_1(d+R)^3 - \frac{4}{3}\pi\rho_1 N_1 R^3 = C_1 V_1(1-e^{-k_1 t}) \quad (1)$$

R is the radius of NDs (assuming NDs are spheres), p_1 is the density of PDA, V_1 is the reaction volume, N_1 is the number of NDs, and k_1 is a constant related to pH values, partial pressure of O_2, ambient temperature and luminous intensity[23]. Therefore, the thickness of a PDA layer can be written as **equation (2)**

$$d = \sqrt[3]{\frac{3C_1V_1(1-e^{-k_1t})+4\pi\rho_1N_1R^3}{4\pi\rho_1N_1}} - R \quad (2)$$

Or if we rewrite **equation (1)** to **(3):**

$$(d+R)^3 - R^3 = d^3 + 3d^2R + 3dR^2 = \frac{3C_1V_1(1-e^{-k_1t})}{4\pi\rho_1N_1} \quad (3)$$

Then, eliminate d^3 and $3d^2R$ because d is far less than R (d<<R).

At last, the *d* can be expressed as **equation (4)**

$$d = \frac{C_1 V_1 (1-e^{-k_1 t})}{4\pi \rho_1 N_1 R^2} \quad (4)$$

The coating process required 12 h, with the DA being completely consumed and monitored by UV-vis spectra. Therefore, $\frac{V_1 (1-e^{-k_1 t})}{4\pi \rho_1 N_1 R^2}$ was a constant, and the value of *d* was directly proportional to the initial concentrations of DA (C_1), which were confirmed by our experimental results (**Table 1**). Please note, along with the increase in the thicknesses of the PDA layers, accumulation speeds of the layers were slower because of the increases in the surface areas of the NDs-PDA.

The presence of the catechol groups in PDA has been shown to directly induce the growth of the nanoparticles upon the reduction of metal precursors and their immobilization on a PDA-coated surface[24,25,26,27]. After coating 100 nm NDs with a PDA layer (~ 15 nm), the resulting PDA-NDs were used as a substrate to synthesize AgNPs from a metal ion solution, with the assistance of sonication. As seen in **Figure 2**, with the increase of $[Ag(NH_3)_2]^+$ concentration, the size of AgNPs increased from ~24 nm to ~28 nm, and the number of NPs raised from 97 to 117, corresponding to the $[Ag(NH_3)_2]^+$ concentration of 0.4 to 0.6 mg/mL, respectively. This phenomenon can also be characterized by UV-vis spectroscopy. The absorbance peak of nanoparticles gradually appeared as the concentration of $[Ag(NH_3)_2]^+$ increased (**Figure 4**). For example, the maximum absorbance of nanoparticles, formed by reducing 0.4 and 0.6 mg/mL of $[Ag(NH_3)_2]^+$, is 410 and 430 nm, which corresponds to AgNPs with the diameters of #20 and #30 nm, respectively. This is consistent with TEM observation[17].

The diameter of reduced AgNPs follows the first order linear differential **equation (5)**, which is similar to the seeded growth synthesis of AuNPs[28], where the *S* is the surface area of PDA-NDs, C_2 is the initial concentrations of $Ag[(NH_3)_2]^+$, *t* is the reaction time, *r* is the radius of AgNPs, k_2 is a constant, p_2 is the density of Ag, V_2 is the reaction volume, N_2 is the number of AgNPs, and equals to $S \cdot n$, in which *n* is the average number of active catechol groups that can reduce $Ag[(NH_3)_2]^+$. The AgNPs are treated as spheres:

$$S \cdot n \cdot \frac{4}{3}\pi\rho_2 r^3 = \frac{4}{3}\pi\rho_2 N_2 r^3 = C_2 V_2 (1-e^{-k_2 t}) \quad (5)$$

In the equation, the number of AgNPs was assumed to be directly proportional to the surface area of PDA, which depended on the thicknesses of the PDA layers. On the surface of the PDA layers, the AgNPs grew with the continuous reduction of $Ag[(NH_3)_2]^+$, while the metal (0) bonds at the O-site of the PDA served as the seed precursor of AgNPs. The number of AgNPs is proportional to the O-site on PDA, which is directly proportional to the surface area[23,29,30,31]. On the other hand, the reduced AgNPs are distributed evenly on the PDA surface because the $Ag[(NH_3)_2]^+$ was reduced by the uniformed catechol groups on the PDA layers. Experimental results showed that the higher the initial concentrations of $Ag[(NH_3)_2]^+$ were, the larger the AgNPs were, but with a similar number of NPs on each ND. The ratio of initial concentrations of $[Ag(NH_3)_2]^+$ (C_2) ratio (0.6 mg/mL : 0.4 mg/mL=1.5) were consistent with the average radius cubed $[(14/12)^3=1.588]$. Therefore, if a higher density of particles is desired on the PDA-NDs, a thicker layer of PDA-NDs should be selected but, if larger sizes of NPs are needed, a longer reduction duration would meet the requirement.

To remove the unreacted $[Ag(NH_3)_2]^+$ during the purification process, a high centrifugation speed is recommended because of the low density of NDs. The higher the centrifugation speed is, the shorter the purification duration will be, which will provide better control of the sizes of AgNPs. In addition, sonication is an indispensable approach for obtaining uniform AgNPs. Samples should be sonicated for several minutes initially before $Ag[(NH_3)_2]^+$ solutions are added.

We have demonstrated a facile method for the surface modification of NDs with self-polymerized PDA. Compared with the Click Chemistry method, this strategy, not only enhances ND dispersity and stability, but also provides a reactive platform (PDA layer) for potential post-modification by reducing the metal nanoparticles or linking with amino/thiol attached species. The thickness of a PDA layer and the size of the nanoparticles on ND surfaces can be changed by varying PDA and $Ag[(NH_3)_2]^+$ concentrations. They can also be used to reduce AuNPs or other noble metal NPs. By combining the diversity of PDA chemistry and the unique properties of NDs, this method will open the door for extending ND's applications in the catalyst, energy, and biomedical areas.

Disclosures

The authors have nothing to disclose.

Acknowledgements

This research was supported by National Science Foundation (CCF 1814797) and University of Missouri Research Board, Material Research Center, and the College of Arts and Science at Missouri University of Science and Technology

References

1. Mochalin, V.N., Shenderova, O., Ho, D., Gogotsi, Y. The properties and applications of nanodiamonds. *Nature Nanotechnology.* **7** (1), 11-23 (2011).
2. Kucsko, G. *et al.* Nanometre-scale thermometry in a living cell. *Nature.* **500** (7460), 54-58 (2013).
3. Liu, J. *et al.* Origin of the Robust Catalytic Performance of Nanodiamond-Graphene-Supported Pt Nanoparticles Used in the Propane Dehydrogenation Reaction. *ACS Catalysis.* **7** (5), 3349-3355 (2017).
4. Chang, B.-M. *et al.* Highly Fluorescent Nanodiamonds Protein-Functionalized for Cell Labeling and Targeting. *Advanced Functional Materials.* **23** (46), 5737-5745 (2013).

5. Ho, D., Wang, C.H., Chow, E.K. Nanodiamonds: The intersection of nanotechnology, drug development, and personalized medicine. *Science Advances.* **1** (7), e1500439 (2015).
6. Hsu, M.H. *et al.* Directly thiolated modification onto the surface of detonation nanodiamonds. *ACS Applied Materials and Interfaces.* **6** (10), 7198-7203 (2014).
7. Krueger, A. Diamond Nanoparticles: Jewels for Chemistry and Physics. *Advanced Materials.* **20** (12), 2445-2449 (2008).
8. Turcheniuk, K., Trecazzi, C., Deeleepojananan, C., Mochalin, V.N. Salt-assisted ultrasonic deaggregation of nanodiamond. *ACS Applied Materials and Interfaces.* **8** (38), 25461-25468 (2016).
9. Akiel, R.D., Zhang, X., Abeywardana, C., Stepanov, V., Qin, P.Z., Takahashi, S. Investigating Functional DNA Grafted on Nanodiamond Surface Using Site-Directed Spin Labeling and Electron Paramagnetic Resonance Spectroscopy. *Journal of Physical Chemistry B.* **120** (17), 4003-4008 (2016).
10. Gaillard, C. *et al.* Peptide nucleic acid-nanodiamonds: covalent and stable conjugates for DNA targeting. *RSC Advances.* **4** (7), 3566-3572 (2014).
11. Zhang, T. *et al.* DNA-based self-assembly of fluorescent nanodiamonds. *Journal of the American Chemical Society.* **137** (31), 9776-9779 (2015).
12. Liu, W. *et al.* Fluorescent Nanodiamond-Gold Hybrid Particles for Multimodal Optical and Electron Microscopy Cellular Imaging. *Nano Letters.* **16** (10), 6236-6244 (2016).
13. Lee, H., Dellatore, S.M., Miller, W.M., Messersmith, P.B. Mussel-inspired surface chemistry for multifunctional coatings. *Science.* **318** (5849), 426-430 (2007).
14. Wang, C., Zhou, J., Wang, P., He, W., Duan, H. Robust Nanoparticle-DNA Conjugates Based on Mussel-Inspired Polydopamine Coating for Cell Imaging and Tailored Self-Assembly. *Bioconjugate Chemistry.* **27** (3), 815-823 (2016).
15. Liu, R., Guo, Y., Odusote, G., Qu, F., Priestley, R.D. Core-shell Fe_3O_4polydopamine nanoparticles serve multipurpose as drug carrier, catalyst support and carbon adsorbent. *ACS Applied Materials and Interfaces.* **5** (18), 9167-9171 (2013).
16. Liu, R. *et al.* Dopamine as a Carbon Source: The Controlled Synthesis of Hollow Carbon Spheres and Yolk-Structured Carbon Nanocomposites. *Angewandte Chemie International Edition.* **50** (30), 6799-6802 (2011).
17. Zeng, Y., Liu, W., Wang, Z., Singamaneni, S., Wang, R. Multifunctional surface modification of nanodiamonds based on dopamine polymerization. *Langmuir.* **34** (13), 4036-4042 (2018).
18. Qin, S. *et al.* Dopamine@Nanodiamond as novel reinforcing nanofillers for polyimide with enhanced thermal, mechanical and wear resistance performance. *RSC Advances.* **8** (7), 3694-3704 (2018).
19. Barras, A., Lyskawa, J., Szunerits, S., Woisel, P., Boukherroub, R. Direct functionalization of nanodiamond particles using dopamine derivatives. *Langmuir.* **27** (20), 12451-12557 (2011).
20. Khanal, M. *et al.* Toward Multifunctional "Clickable" Diamond Nanoparticles. *Langmuir.* **31** (13), 3926-3933 (2015).
21. Rad, M.H., Zamanian, A., Hadavi, S.M.M., Khanlarkhani A. A Two-Stage Kinetics Model for Polydopamine Layer Growth. A Two-Stage Kinetics Model for Polydopamine Layer Growth. *Macromolecular Chemistry and Physics.* 1700505 (2018).
22. Ball, V., Frari, D.D., Toniazzo, V., Ruch, D.Kinetics of polydopamine film deposition as a function of pH and dopamine concentration: Insights in the polydopamine deposition mechanism. *Journal of Colloid and Interface Science*. **386** (1), 366-372 (2012).
23. Liu, Y., Ai, K., Lu, L. Polydopamine and its derivative materials: synthesis and promising applications in energy, environmental, and biomedical fields. *Chemical Reviews.* **114** (9), 5057-5115 (2014).
24. Hu, J., Wu, S., Cao, Q., Zhang, W. Synthesis of core-shell structured alumina/Cu microspheres using activation by silver nanoparticles deposited on polydopamine-coated surfaces. *RSC Advances.* **6** (85), 81767-81773 (2016).
25. Orishchin, N. *et al.* Rapid Deposition of Uniform Polydopamine Coatings on Nanoparticle Surfaces with Controllable Thickness. *Langmuir.* **33** (24), 6046-6053 (2017).
26. González, A.L., Noguez, C., Beránek, J., Barnard, A.S. Size, Shape, Stability, and Color of Plasmonic Silver Nanoparticles. *Journal of Physical Chemistry C.* **118** (17), 9128-9136 (2014).
27. Muthuchamy, N., Gopalan, A., Lee, K.-P. A new facile strategy for higher loading of silver nanoparticles onto silica for efficient catalytic reduction of 4-nitrophenol. *RSC Advances.* **5** (93), 76170-76181 (2015).
28. Bastus, N.G., Comenge, J., Puntes, V. Kinetically Controlled Seeded Growth Synthesis of Citrate-Stabilized Gold Nanoparticles of up to 200 nm: Size Focusing versus Ostwald Ripening. *Langmuir.* **27** (17), 11098-11105 (2011).
29. Jana, J., Gauri, S.S., Ganguly, M., Dey, S., Pal, T. Silver nanoparticle anchored carbon dots for improved sensing, catalytic and intriguing antimicrobial activity. *Dalton Transactions.* **44** (47), 20692-20707 (2015).
30. Zamudio, A. *et al.* Efficient anchoring of silver nanoparticles on N-doped carbon nanotubes. *Small.* **2** (3), 346-350 (2006).
31. Chen, K., Li, T. Modification of membranes with polydopamine and silver nanoparticles formed *in situ*. to mitigate biofouling. *U.S. Patent Application.*14/689,085 (2016).

